

Statistical validation of GCM-simulated climates for the U.S. Great Lakes and the C.I.S. Emba and Ural River basins

V. Privalsky

Inst. of Applied Astronomy, Russian Academy of Sciences, Zheanovskaya No. 8,
St. Petersburg, Russia 197042

T. E. Croley II

Great Lakes Environmental Research Laboratory, NOAA, 2205 Commonwealth Blvd.,
Ann Arbor, MI 48105-1593, USA

Abstract: Many researchers use outputs from large-scale global circulation models of the atmosphere to assess hydrological and other impacts associated with climate change. However, these models cannot capture all climate variations since the physical processes are imperfectly understood and are poorly represented at smaller regional scales. This paper statistically compares model outputs from the global circulation model of the Geophysical Fluid Dynamics Laboratory to historical data for the United States' Laurentian Great Lakes and for the Emba and Ural River basins in the Commonwealth of Independent States (C.I.S.). We use maximum entropy spectral analysis to compare model and data time series, allowing us to both assess statistical predictabilities and to describe the time series in both time and frequency domains. This comparison initiates assessments of the model's representation of the real world and suggests areas of model improvement.

Key words: Hydrology, global circulation models, statistics, climate change.

1 Introduction

Large-scale general circulation models (GCMs) of the earth's atmosphere are being used to simulate climate changes, typically over a few decades, and to estimate hydrological impacts associated with various climate changes. Climate scenarios, developed from different GCMs, are used to assess changes in the properties of hydrological parameters caused by anthropogenically-induced climate change; see USEPA (1984, 1988), Cohen (1986, 1987), and Croley (1990). Recently, the Water Problems Institute, the Soviet Geophysical Committee, and the Great Lakes Environmental Research Laboratory started a cooperative U.S.S.R. - U.S. project to assess hydrological impacts of climate change over the Caspian Sea Basin.

The GCMs produce daily values of major meteorological parameters (air temperature and pressure, precipitation, run-off, etc.) at the nodes of grids defined at approximately 4 to 8 degrees latitude by 5 to 10 degrees longitude. Although the quality of climate reproduction that can be achieved with these models still is insufficient, many researchers modify historical data sets with GCM scenarios and use these data sets with detailed regional models to predict both natural and anthropogenic changes of climate. These models can give erroneous pictures of mean spatial distributions of

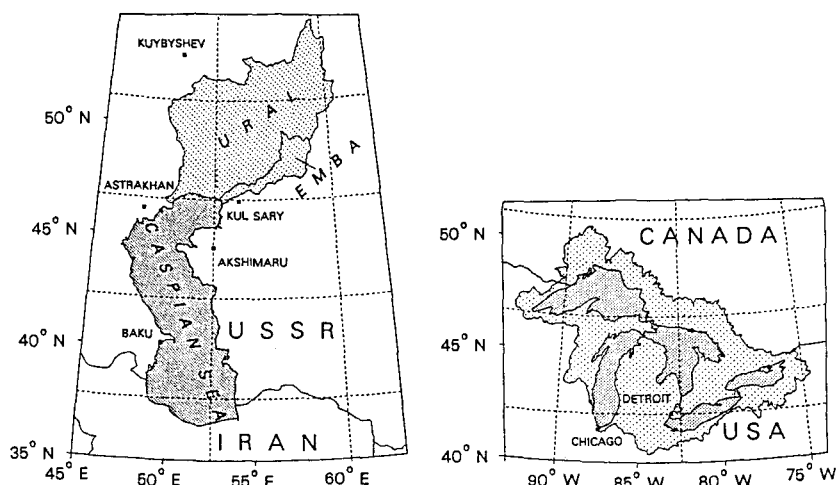


Figure 1. Location and GCM gridpoints for the Emba and Ural River basins and the U.S. Great Lakes basin

major climatic parameters, such as air pressure, over large portions of the northern hemisphere (Wigley and Santer, 1988). Corrections can consist of improved coupling of atmospheric and oceanic models, faster computers, and higher spatial resolution, as well as other physical and numerical means. Hopefully, this will lead eventually to models capable of a much better reproduction of the actual spatial distribution of major climatic parameters.

However, improved models never can capture all temporal variations in climate since there is inherent stochasticity in the physical processes with respect to current scientific knowledge of these processes (WMO, 1975). Furthermore, a model's ability to give an accurate average picture of climate does not mean necessarily that it correctly describes climatic variability. Finally, there is some question of the applicability of GCMs to regional-scale studies.

By comparing statistical properties of actual and GCM-simulated climates, we may verify the model's representation of nature and suggest areas of model improvement for further research. This paper describes this comparison for the Geophysical Fluid Dynamics Laboratory (GFDL) GCM and two regions: the Emba and Ural River basins in Russia and Kazakhstan, and the basin of the Laurentian Great Lakes in the North American continent (Fig. 1).

2 Data sets

Actual historical meteorology and GCM-simulated time series of monthly air temperature and precipitation are compared for the Great Lakes basin, in the United States, and the basins of the Emba and Ural Rivers, in Russia and Kazakhstan.

Daily precipitation and minimum and maximum daily air temperatures are available from 1,569 stations for the Laurentian Great Lakes basin (covering a land area of about 522,000 km²) between 1900-88 and from 58 stations for the Emba and Ural river basins (covering a combined area of over 377,000 km²) between 1955-76. The data for the Great Lakes were obtained from the U.S. National Climatic Data Center, and the Russian and Kazakhstan basin data were obtained from The All-Union

Research Institute of Hydrometeorological Information, World Data Center B. These data were reduced to daily areal averages over these basins through Thiessen averaging (Croley and Hartmann, 1985, 1986; Croley and Ferronsky, 1990a,b). Consistency

checks were performed to identify and correct data errors in the records (Croley et al., 1991). Data availability appears very good for these basins. The Great Lakes basin data set was truncated to the same 22 years available for the Emba and Ural Basins (Emba/Ural basin) to allow direct comparisons between the two sets of data. Both daily time series were reduced to monthly data, after a preliminary statistical analysis, to agree with the available GCM output format.

The GCM used here was developed at the Geophysical Fluid Dynamics Laboratory (Manabe and Wetherald, 1987) and used to simulate, for present-day CO_2 concentrations, 10 years of daily maximum and minimum air temperature and daily precipitation (among other variables); see Jenny (1988). This GCM has a spatial resolution of 4.4° latitude by 7.5° longitude (about 520 km by 510 km at $45^\circ N$ latitude). The model's grid points are depicted in Fig. 1.

3 Properties to be compared

Besides major statistical parameters such as mean and root mean square (RMS) values, we compare the following statistical characteristics of the actual and simulated monthly air temperature and precipitation time series for each basin: i) sample probability distributions, ii) seasonal trends, iii) spectral densities and, whenever practical, autoregressive (AR) models in the time domain, and iv) parameters of statistical predictability. Daily air temperature is taken as the average of the daily maximum and minimum air temperatures. Seasonal trends in all time series are estimated by averaging values for each month of the year, and the time series resulting by subtraction of seasonal trends are referred to as "deseasonalized" in what follows.

The time series are relatively short (264 months for the actual and 120 months for the simulated time series). This means that traditional techniques of spectral analysis will give statistically unreliable results. Therefore, we apply maximum entropy spectral analysis, which is designed to analyze relatively short time series. It has two other advantages especially useful for this study. First, it leads to an immediate and simple solution of the least-squares prediction problem inside the framework of the Kolmogorov-Wiener theory, thus enabling us to assess statistical predictability of our processes. Second, as the technique is based upon fitting autoregressive (AR) models to the time series, it gives simultaneous description of the time series in both the frequency and time domains (spectral density and respective linear stochastic difference equations). For a thorough description of the theory of this approach see Yaglom (1987).

Four criteria are used to choose the best AR-approximation to the time series: Akaike's information criteria (AIC), Parzen's CAT, Schwarz-Rissanen's BIC, and Hannan-Quinn's HQ. In those cases where different criteria indicate different AR orders for the same time series, the AIC is used as a rule. Models containing the moving-average operator were not studied because of their computational instability (Privalsky, 1985; Yaglom, 1987).

The parameters of statistical predictability include the relative prediction error (RPE) at one step (one month) lead time and the limit of statistical predictability (LISP). Their meaning is explained below.

Consider an autoregressive model of order p for time series x_t with AR coefficients ϕ_i :

$$x_t = \sum_{i=1}^p \phi_i x_{t-i} + a_t \quad (1)$$

where a_t is a sequence of (mutually) independent identically distributed random vari-

ables and t is time. The spectrum of x_t is found as

$$s_{xx}(f) = 2\sigma_a^2 \left| 1 - \sum_{i=1}^p \phi_i e^{-2\pi i f \Delta t} \right|^{-2}, \quad 0 \leq f \leq \frac{1}{2} \Delta t \quad (2)$$

where σ_a^2 is the variance of a_t and Δt is the time increment between successive values of x_t (Box and Jenkins, 1970). The least-squares prediction $\hat{x}_t(\tau)$ of x_t at lead time τ starting at t is

$$\hat{x}_t(\tau) = \sum_{i=1}^p \phi_i \hat{x}_t(\tau - i) \quad (3)$$

where $\hat{x}_t(\tau - i) = x_{t-i}$ for $t \leq i$. Thus, a_t is the prediction error and σ_a^2 is its variance, at the unit lead time, $\tau = 1$. Its ratio to the time series variance

$$d_p(1) = \sigma_a^2 / \sigma_x^2 \quad (4)$$

is called the (one-step) relative prediction error (RPE).

Obviously, the prediction error at lead time τ is $\delta_p(\tau) = x_{t+\tau} - x_t(\tau)$, and it can be easily shown (see Box and Jenkins, 1970) that the prediction error variance is

$$D_p(\tau) = \sigma_a^2 \sum_{i=0}^{\tau-1} \beta_i^2$$

where β_i are the coefficients of the inverse autoregressive operator. In the stationary case, which is the case considered here, the variance $D_p(\tau)$ tends to σ_x^2 as τ tends to infinity. Thus, RPE

$$d_p(\tau) = D_p(\tau) / \sigma_x^2 \quad (5)$$

lies between zero (singular process) and unity (purely random process, or white noise).

Note that the correlation coefficient $r_p(\tau)$ between the actual value of the time series and its prediction at lead time τ can be found as

$$r_p^2(\tau) = 1 - d_p(\tau).$$

Finally, the limit of statistical predictability (LISP) τ_α , of time series x_t , is defined as the lead time τ , at which RPE reaches a prespecified value $\alpha \approx 1$. We will assume $\alpha = 0.9$. This value also is called predictability horizon (Privalsky, 1985, 1988).

Equations (4), (5), and LISP $\tau_{0.9}$ define the measures of statistical predictability used in this study to compare the properties of the actual and simulated climatic time series. They all describe the persistence of the time series. Note that the actual predictability will be smaller because we only have estimates of AR parameters p , ϕ_i , and σ_a^2 (Box and Jenkins, 1970). However, this fact is of no importance to us because the criteria of predictability are used only to describe statistical properties of our time series. Actual predictions will not be made here because of their low accuracy.

4 Comparisons

Since we have only 10 years of simulated climate but 22 years of actual observations, we will compare these time series of different lengths rather than breaking the actual time series into two series of 11 years each. Two types of comparisons are made for time series with and without seasonal trends: first, we compare the data sets as samples of random variables (that is, estimate the probability density functions and their parameters) and then we compare them as sample records of random processes

(seasonal trends, spectral densities, predictability parameters) inside the framework of linear AR models with constant parameters. [Actually, multiplicative AR models (Box and Jenkins, 1970),

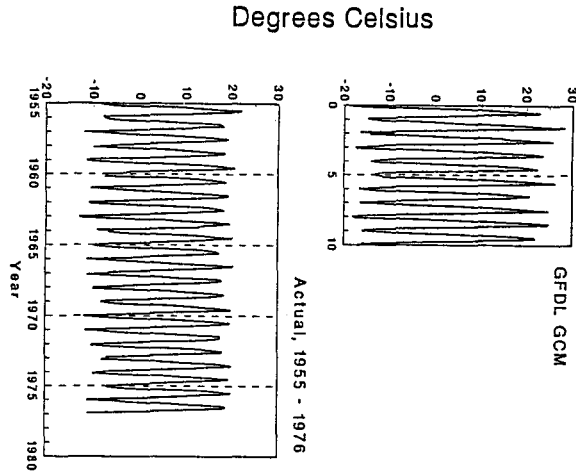


Figure 2. Actual and GCM-simulated mean monthly air temperatures in the U.S. Great Lakes basin

$$(1 - \Phi_1 B^{12} - \dots - \Phi_P B^{12P})(1 - \phi_1 B - \dots - \phi_p B^p)x_t = a_t$$

have also been analyzed for all our time series but we decided not to include them into this study because they give a seasonal trend more regular than observed in the time series.]

4.1 Air temperature

As seen from Fig. 2, the GCM-simulated air temperature in the Great Lakes basin behaves in about the same manner as the actual temperature with more range in the modeled time series. This is also true for the Emba/Ural basin (not shown). This observation is documented by respective estimates of mean and RMS values (Table 1). As seen from the table, mean and RMS values for the actual and simulated air temperature do not differ much both before and after deseasonalizing for both basins. They also have about the same predictability parameters RPE $d_p(1)$ and LISP $\tau_{0.9}$. Although different criteria may lead to different models for any particular time series, respective values for predictability parameters (shown in parentheses in Table 1 for criteria other than AIC) do not differ drastically. Thus, for the Emba/Ural basin time series of air temperature, the AIC indicates an AR model of order $p = 26$ while the BIC indicates $p = 12$; however, respective RPEs differ by just 0.6% (4.5% versus 5.1%) with both LISPs exceeding 100 months. The mean and RMS values of the actual and simulated air temperature are statistically equivalent at the 95% significance level (see Table 2).

Another important factor is the shape of the sample probability distribution functions for the actual and simulated time series of air temperature. To avoid effects related to differences in sample mean values and variances, the time series were transformed to zero mean and unit variance before comparisons. Then the Kolmogorov-Smirnov two-sample test were used to compare the shapes of the cumulative distribution functions (CDFs) of the actual and simulated air temperatures. The comparisons showed that the shapes of the CDFs of these transformed actual and simulated data differ significantly only for non-deseasonalized air temperature in the Emba/Ural basin (see Table 2), suggesting that the seasonal trend is not reproduced correctly by

Table 1. Comparison of actual and simulated climate mean monthly air temperature

		Mean Value °C	RMS °C	p	$d_p(1)$ %	$\tau_{0.9}$ months
<i>Emba/Ural basin</i>						
Raw data:	Actual	5.3	13.4	26 (12, 21) ^a	4.5 (5.1, 4.7)	> 100
	GCM	6.5	13.6	11	6.3	> 100
Deseasonalized:	Actual		2.5	1	96	1
	GCM		2.6	12 (1)	82 (90)	2 (1)
<i>Great Lakes basin</i>						
Raw data:	Actual	5.5	10.2	20 (16, 8)	3.3 (3.4, 3.7)	> 100
	GCM	3.6	14.3	12	3.3	> 100
Deseasonalized:	Actual		1.66	25 (0, 1)	88 (99)	4 (0)
	GCM		2.13	1	96	0

^aPredictability parameters for criteria other than AIC are shown in parentheses

Table 2. Hypotheses rejection (R) or non-rejection (A) of equivalence between historical and GCM parameters at 95% significance level

Parameter	Air Temperature				Precipitation			
	Emba/Ural		Great Lakes		Emba/Ural		Great Lakes	
	Raw Data	Deseas.	Raw Data	Deseas.	Raw Data	Deseas.	Raw Data	Deseas.
Mean	A		A		R		R	
Variance	A	A	A	A	R	R	A	A
C.D.F.	R	A	A	A	A	A	A	A

the GCM for this basin. The results of the comparisons shown in Table 2 also suggest that the GCM simulates time series of mean monthly air temperature with acceptable mean and variance values both before and after the seasonal cycle is removed on both the Great Lakes and the Emba/Ural basins.

Now, even when actual and simulated temperature data, regarded as samples of *random variables*, do coincide statistically, that does not mean that the model successfully reproduces climatic parameters as *random processes*. To check its adequacy in this respect, we compared spectral densities and predictability parameters of the actual and simulated time series. The spectra of mean monthly air temperature, shown in Fig. 3 for the Emba/Ural basin, correspond to AR models of order $p = 26$ for the actual and $p = 11$ for the simulated time series. Figure 3 also shows spectra for mean monthly air temperature in the Great Lakes basin corresponding to AR models with $p = 20$ for the actual and $p = 12$ for the simulated time series. These are the autoregressive models identified in Table 1. The spectra reveal strong peaks at the seasonal trend frequency $f = 1.0$ cycle per year (cpy) and at its higher harmonics for all time series.

The range of the seasonal trend seems to be greater in the simulated time series for both basins (see Fig. 2). Indeed, the difference between the average ranges in the simulated and actual average seasonal trends amounts to only 2°C in the Emba/Ural basin (the average ranges of actual and simulated mean seasonal trends are 36°C and

38°C respectively) and to 11°C in the Great Lakes basin (28°C and 39°C respectively). The latter figure looks quite impressive. The seasonal extremes of air temperature are reproduced by the GCM reasonably except for the seasonal maximum in the Great

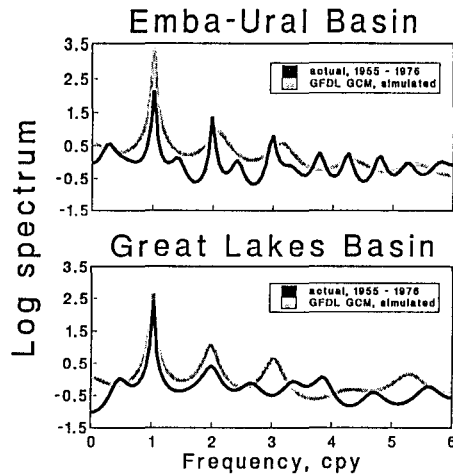


Figure 3

Figure 3. Spectra of actual and GCM-simulated monthly air temperatures in the Emba-Ural and the U.S. Great Lakes basins

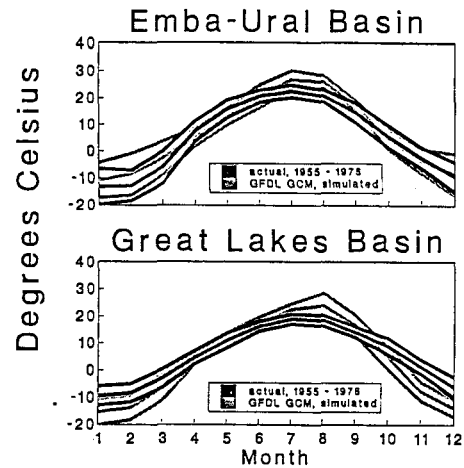


Figure 4

Figure 4. Average seasonal trend and 90% confidence limits in monthly air temperature on the Emba-Ural and the U.S. Great Lakes basins

Lakes basin, which is shifted from July to August (see Fig. 4). Note that the middle lines in Fig. 4 correspond to the average seasonal trends while the other two lines show the respective 90% confidence limits.

As seen from Fig. 4, the model generates time series of air temperature with about the same degree of regularity in summer but less distinct in winter. The 90% confidence bands for the estimates of seasonal trend are wider in the simulated series by 2 or 3°C in winter time for both basins. The confidence bands for the seasonal trends in the actual and simulated temperature overlap for all months except November and December in the Great Lakes basin. This means that the differences in seasonal trends between the actual and simulated data are mostly insignificant statistically. Naturally, the seasonal trend is greater and more variable in the Emba/Ural basin due to its sharply continental climate.

The regularity of the seasonal trend in the actual and simulated time series of temperature is also seen from the form of the respective spectra. Quantitative estimates can be obtained by analyzing statistical predictability parameters. Obviously, for any process with a strong predominance of seasonal trend, RPE $d_p(1)$ should be very small, with LISP $\tau_{0.9}$ extending to many months. Indeed, this is what happens for both the Emba/Ural basin and the Graet Lakes basin ($\tau_{0.9}$ exceeds 100 months, see Table 1). However, in the Emba/Ural basin the seasonal trend seems to be more blurred in the simulated series than in the actual one because RPE $d_p(\tau)$ increases much faster for the former series (see Fig. 5). In the Great Lakes basin, the simulated and actual time series possess about the same regularity in their seasonal trend (see Fig. 5). Finally, the seasonal cycle in the simulated series is less regular in the Emba/Ural basin than in the Great Lakes basin while, for actual temperatures, their predictability properties are very similar (bottom curves in Fig. 5).

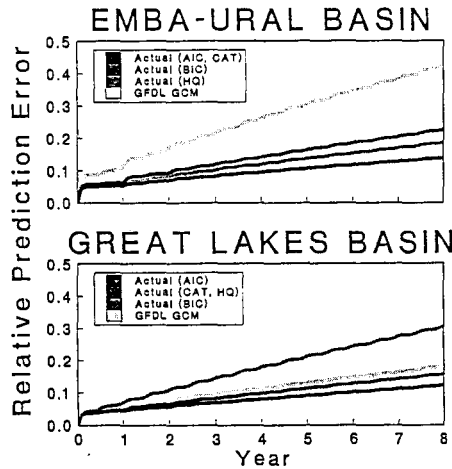


Figure 5

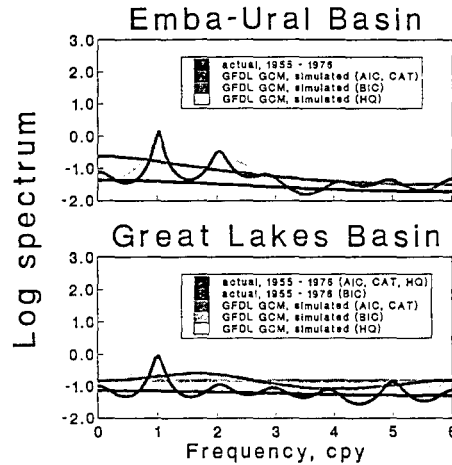


Figure 6

Figure 5. Relative prediction error $d_p(\tau)$ for monthly air temperatures on the Emba-Ural and the U.S. Great Lakes basins

Figure 6. Spectra of actual and GCM-simulated deseasonalized monthly air temperatures and selected AR models for the Emba-Ural and the U.S. Great Lakes basins with selected trends removed

When the seasonal trends are removed from Fig. 2 (not shown), both the simulated and actual air temperatures behave almost as white noise. Figure 6 shows spectra of deseasonalized time series and selected AR models of those deseasonalized time series chosen according to different criteria. Thus, the two spectra identified as GCM (AIC, CAT) and GCM (BIC, HQ) in Fig. 6 represent AR models of the same time series of deseasonalized GCM-simulated monthly air temperature in the Emba/Ural basin according to the AIC and CAT or to the BIC and HQ criteria, respectively. The fact that the processes that correspond to the peaked and monotonic spectra in Fig. 6 are quite similar is seen from the values of $d_p(1)$ and $\tau_{0.9}$ given in Table 1 for deseasonalized temperature in both basins. In all cases, the deseasonalized time series spectra is indistinguishable from white noise in Fig. 6.

The deseasonalized time series of actual temperature in the Emba/Ural basin is approximated with an AR model

$$T_t = 0.21T_{t-1} + a_t, \quad (\text{RMSE of parameter estimate} = 0.06) \quad (6)$$

with $\sigma_a = 2.5^\circ\text{C}$ while the best AR model for the simulated series is

$$\hat{T}_t = 0.32\hat{T}_{t-1} + \hat{a}_t, \quad (\text{RMSE of parameter estimate} = 0.09) \quad (7)$$

with $\hat{\sigma}_a = 2.7^\circ\text{C}$. The difference between these two models is statistically insignificant.

For the Great Lakes basin, the models of deseasonalized actual and simulated temperature are quite similar.

$$T_t = 0.12T_{t-1} + a_t, \quad (\text{RMSE of parameter estimate} = 0.06) \quad (8)$$

$$\hat{T}_t = 0.13\hat{T}_{t-1} + \hat{a}_t, \quad (\text{RMSE of parameter estimate} = 0.09) \quad (9)$$

Table 3. Comparison of actual and simulated climate mean monthly precipitation

		Mean Value mm d ⁻¹	RMS mm d ⁻¹	p	$d_p(1)$ %	$\tau_{0.9}$ months
<i>Emba/Ural basin</i>						
Raw data:	Actual	0.76	0.41	1	96	1
	GCM	1.40	0.72	12 (1, 7) ^a	64 (79, 69)	13 (2, 5)
Deseasonalized:	Actual		0.39	1	98	0
	GCM		0.51	1	95	1
<i>Great Lakes basin</i>						
Raw data:	Actual	2.2	0.73	12 (1)	79 (100)	12 (0)
	GCM	3.0	0.95	3 (0, 1)	96 (98)	0
Deseasonalized:	Actual		0.60	1 (0)	99	0
	GCM		0.82	0	100	0

^aPredictability parameters for criteria other than AIC are shown in parentheses

with $\sigma_a = 1.6^\circ C$ and $\hat{\alpha}_a = 2.1^\circ C$. Note that the models are very close to white noise and therefore have almost zero predictability (see Table 1).

4.2 Precipitation

The GFDL GCM appears to be rather poor in simulating precipitation in both the Emba/Ural basin and the Great Lakes basin and is strongly biased (see Table 3). The hypothesis of equal mean values for the actual and simulated precipitation time series is rejected for both basins (see Table 2). Yet, according to Table 2, the variances in the Great Lakes basin differ insignificantly and the model seems to be able to reproduce the *shape* of the probability distribution functions for both basins.

Seasonal patterns of precipitation do not appear in these basins and attempts to depict average seasonal precipitation behaviour (as in Fig. 4 for air temperature) are quite irregular; see Fig. 7. In agreement with the actual data, the cycle is rather irregular in the simulated series as well but it has larger amplitude and variance and its peaks do not agree with the actual data. The differences in the trend's shape and its regularity are large, especially for the Emba/Ural basin. However, it seems important to us that the model has revealed capability to differ between processes with strong and weak seasonal cycles (air temperature versus precipitation; see Figs. 4 and 7).

The irregularity in the seasonal trend in the Emba/Ural basin is revealed clearly in the spectrum estimates for precipitation in Fig. 8. The weak seasonal trend in the actual Emba/Ural basin precipitation leads to a very flat spectrum, while two out of the three spectrum estimates for the simulated data contain shape peaks at $f = 1$ cpy (see Fig. 8).

The actual time series is approximated with the AR(1) model,

$$P_t = 0.20P_{t-1} + a_t, \quad (RMSE \text{ of parameter estimate} = 0.06) \quad (10)$$

where $\sigma_a^2 = 0.17 (mm/day)^2$ while the best approximation for the simulated series is an AR model of order $p = 12$, which gives a strong seasonal cycle (maximum peak in Fig. 8) and differs significantly from (10). Specifically, the predictability of the simulated series is higher than that of the actual precipitation (compare values of $d_p(1)$ and $\tau_{0.9}$ for the actual and simulated Emba/Ural basin precipitation in Table 3). Thus, the GCM simulation of precipitation in the Emba/Ural basin should be regarded as unsuccessful from this point of view.

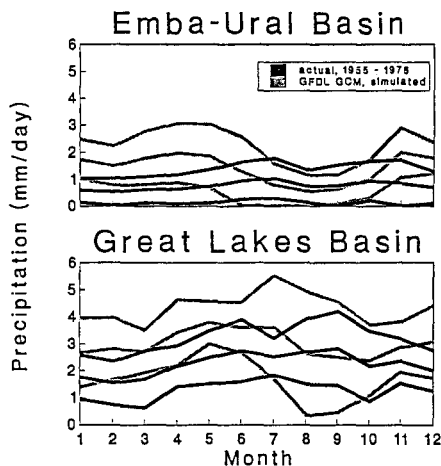


Figure 7

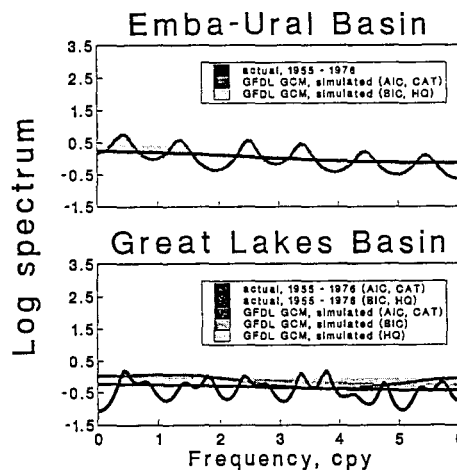


Figure 8

Figure 7. Average seasonal trend and 90% confidence limits in monthly precipitation on the Emba-Ural and the U.S. Great Lakes basins

Figure 8. Spectra of actual and GCM-simulated monthly precipitation in the Emba-Ural and the U.S. Great Lakes basins

In the Great Lakes basin, on the contrary, the actual seasonal trend is more prominent than in the simulated data (see Fig. 8). Although there is a pair of similar spectrum estimates for the actual and simulated precipitation in both basins, diagnostic checking, according to Box and Jenkins (1970), shows that the low-order models with flat spectra should be rejected. The predictability properties of the best-fitting AR models for the actual and simulated time series of precipitation in the basins are dissimilar (see Fig. 9).

When the seasonal trend is removed, the remaining time series have approximately the same properties in each basin. The deseasonalized time series of actual precipitation in the Emba/Ural basin is approximated with an AR model.

$$P_t = 0.15P_{t-1} + a_t, \quad (RMSE \text{ of parameter estimate} = 0.06) \quad (11)$$

with $\sigma_a = 0.38 \text{ mm/day}$ while the best model for the simulated series is

$$\hat{P}_t = 0.20\hat{P}_{t-1} + a_t, \quad (RMSE \text{ of parameter estimate} = 0.09) \quad (12)$$

with $\hat{\sigma}_a = 0.49 \text{ mm/day}$. The difference between these two models is statistically insignificant.

The deseasonalized time series of actual and simulated precipitation in the Great Lakes basin are approximated with AR models of order one, which are both very close to white noise and have statistically equivalent variance estimates (see Table 2). Note, however, that the removal of the seasonal trend from the precipitation time series is hardly necessary because of its irregularity.

Conclusions

The available data sets in this comparative study are not sufficient to arrive at reliable general conclusions concerning statistical adequacy or inadequacy of general

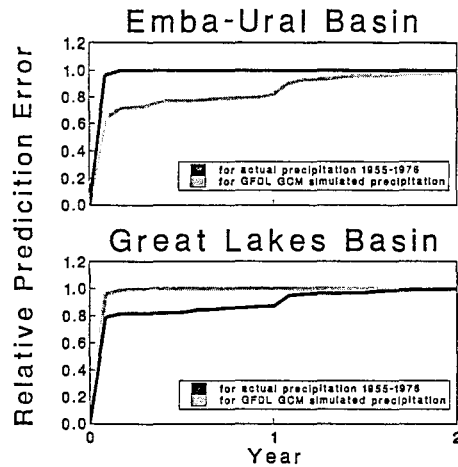


Figure 9. Relative prediction error $d_p(\tau)$ for monthly precipitation on the Emba-Ural and the U.S. Great Lakes basins

circulation models. This attempt to compare major statistical properties of the actual and simulated climates serves as a starting point for more thorough studies to help improve physical models of climate.

The following conclusions can be drawn concerning statistical adequacy of the GFDL general circulation model air temperature and precipitation in the basins of the Emba and Ural Rivers, and the U.S. Great Lakes. First, the model gives correct estimates of mean monthly air temperature and its variance in the basins both before and after seasonal trend is removed and gives acceptable estimates of its probability distribution function for the Great Lakes basin.

The *shape* of the seasonal cycle of air temperature is reproduced reasonably but appears biased positively for both basins in July and August. The model gives less persistent time series of air temperature in both basins before the trend is removed and about the same type of "almost white noise" deseasonalized time series as the actual temperature. However, the discrepancy is not very prominent, at least for the Great Lakes basin.

The model's adequacy concerning monthly precipitation in these two regions is low. It overestimates mean values and variances (the latter is true for the Emba/Ural basin but not for the Great Lakes basin) and gives wrong seasonal trends, spectra, and predictability parameters. This conclusion agrees with common opinion concerning GCM-simulated precipitation. Yet, the model generates time series with approximately correct *shape* in their residual CDFs and, in agreement with actual data, the simulated precipitation has a much weaker seasonal trend and smaller statistical predictability than air temperature.

Acknowledgment

The authors thank Dr. Roy Jenny of the U.S. National Center of Atmospheric Research for providing the GFDL GCM data and to Dr. Sergei Ferronsky of the Russian Geophysical Committee for his help in providing the data for the Emba and Ural basins. This study was supported by GLERL in their joint Russian-American project on the impacts of climate change upon the hydrology of large lake basins, a part of Task 13.01-9 of the US-USSR

Working Group VIII under the joint US-USSR Agreement of Cooperation in Environmental Protection.

References

- Box, G. E. P.; Jenkins, G. M. 1976: Time series analysis: Prediction and control. Holden-Day, New York
- Chevrin, R. M. 1986: Interannual variability and seasonal climate predictability. *J. Atmos. Sci.* 43, 233-251
- Cohen, S. J. 1986: Impacts of CO_2 -induced climatic change on water resources in the Great Lakes basin. *Climatic Change* 8, 135-153
- Cohen, S. J. 1987: Sensitivity of water resources in the Great Lakes region to changes in temperature, precipitation, humidity, and wind speed. Proceedings of the Symposium, The Influence of Climate Change and Climatic Variability on the Hydrologic Regime and Water Resources, IAHS Publ. No. 168, Vancouver, August 1987, pp. 489-499
- Croley, T. E., II 1990: Laurentian Great Lakes Double- CO_2 climate change hydrological impacts. *Climatic Change* 17, 27-47
- Croley, T. E., II; Hartmann, H. C. 1985: Resolving Thiessen polygons. *Journal of Hydrology* 76, 363-379
- Croley, T. E., II; Hartmann, H. C. 1986: Mapping drainage areas on digital maps from boundary coordinates. GLERL Open File Report No. 501, Ann Arbor, 31 pp.
- Croley, T. E., II; Ferronsky, S. V. 1990a: Climate change impacts on the hydrology of the Caspian Sea, 1: Building digital maps of the hydrological basins. Report of the Water Problems Institute, Soviet Geophysical Committee, Moscow, 43 pp. (in Russian)
- Croley, T. E., II; Ferronsky, S. V. 1990b: Climate change impacts on the hydrology of the Caspian Sea, 2: Areal averaging of point meteorological measurements. Report of the Water Problems Institute, Soviet Geophysical Committee, Moscow, 130 pp. (in Russian)
- Croley, T. E., II; Ferronsky, S. V.; Privalsky, V.; Semenov, V. U. 1991: Climate change impacts on the hydrology of the Caspian Sea, 3: Hydrometeorological data on the Emba and Ural river basins. Report of the Water Problems Institute, Soviet Geophysical Committee, Moscow, (in Russian, in press)
- Jenny, R. L. 1988: Data from climate models: The CO_2 warming. NCAR Open File Report, National Center for Atmospheric Research, Boulder
- Manabe, S.; Wetherald, R. T. 1987: Large-scale changes in soil wetness induced by an increase in carbon dioxide. *J. Atmos. Sci.* 44, 1211-1235
- Privalsky, V. E. 1985: Climatic variability: Stochastic models, predictability, and spectra. Nauka, Moscow, 184 pp. (in Russian)
- Privalsky, V. E. 1988: Stochastic models and spectra of interannual variability of mean annual sea surface temperature in the North Atlantic. *Dynam. Atmos. and Oceans* 12, 1-18
- U.S. Environmental Protection Agency 1984: Potential climatic impacts of increasing atmospheric CO_2 with emphasis on water availability and hydrology in the United States. EPA Office of Policy, Planning, and Evaluation, Washington, D. C.
- U.S. Environmental Protection Agency 1988: The Potential effects of global climate change on the United States. Draft report to Congress. Smith, J. B.; Tirpak, D. A. (Eds.), EPA Office of Policy, Planning, and Evaluation, Washington, D. C.
- Wigley, T. M. L.; Santer, B. D. 1988: Validation of general circulation climate models. In: Schlesinger, M. E. (Ed.) *Physically-based modelling and simulation of climate and climatic change*. NATO ASI Series, Kluwer Academic Publishers, Dordrecht, 243, 841-879
- World Meteorological Organization 1975: *The physical basis of climate and climate modeling*. GARP Publication Series No. 16, World Meteorological Organization, Geneva
- Yaglom, A. M. 1987: Correlation theory of stationary random functions. Vols. I (526 pp.) and II (258 pp.). Springer-Verlag, New York

Accepted November 19, 1991